Apolipophorin III interaction with model membranes composed of phosphatidylcholine and sphingomyelin using differential scanning calorimetry

ARTICLE *in* BIOCHIMICA ET BIOPHYSICA ACTA · AUGUST 2009

Impact Factor: 4.66 · DOI: 10.1016/j.bbamem.2009.07.020 · Source: PubMed

4 AUTHORS, INCLUDING:

Chung ping Wan
Celator® Pharmaceuticals
11 PUBLICATIONS **130** CITATIONS
SEE PROFILE

Elmar J Prenner
The University of Calgary
75 PUBLICATIONS **2,111** CITATIONS
SEE PROFILE

Published in final edited form as:
Biochim Biophys Acta. 2009 October ; 1788(10): 2160–2168. doi:10.1016/j.bbamem.2009.07.020.

Apolipophorin III Interaction with Model Membranes Composed of Phosphatidylcholine and Sphingomyelin using Differential Scanning Calorimetry

Michael H Chiu[1], **Chung-Ping Leon Wan**[2], **Paul M.M. Weers**[2], and **Elmar J. Prenner**[1,*]

[1]Department of Biological Sciences, University of Calgary, Calgary, AB, Canada

[2]Department of Chemistry and Biochemistry, California State University, Long Beach, CA, USA

Abstract

Apolipophorin III (apoLp-III) from *Locusta migratoria* was employed as a model apolipoprotein to gain insight into binding interactions with lipid vesicles. Differential scanning calorimetry (DSC) was used to measure the binding interaction of apoLp-III with liposomes composed of mixtures of 1,2-dimyristoyl-sn-glycero-3-phosphocholine (DMPC) and sphingomyelin (SM). Association of apoLp-III with multilamellar liposomes occurred over a temperature range around the liquid crystalline phase transition (L_α). Qualitative and quantitative data were obtained from changes in the lipid phase transition upon addition of apoLp-III. Eleven ratios of DMPC and SM were tested from pure DMPC to pure SM. Broadness of the phase transition ($T_{1/2}$), melting temperature of the phase transition (Tm) and enthalpy were used to determine the relative binding affinity to the liposomes. Multilamellar vesicles composed of 40% DMPC and 60% SM showed the greatest interaction with apoLp-III, indicated by large $T_{1/2}$ values. Pure DMPC showed the weakest interaction and liposomes with lower percentage of DMPC retained domains of pure DMPC, even upon apoLp-III binding indicating demixing of liposome lipids. Addition of apoLp-III to rehydrated liposomes was compared to codissolved trials, in which lipids were rehydrated in the presence of protein, forcing the protein to interact with the lipid system. Similar trends between the codissolved and non-codissolved trials were observed, indicating a similar binding affinity except for pure DMPC. These results suggested that surface defects due to non-ideal packing that occur at the phase transition temperature of the lipid mixtures are responsible for apolipoprotein-lipid interaction in DMPC/SM liposomes.

Keywords

apolipophorin; apolipoprotein; DSC; sphingomyelin; phosphatidylcholine; protein-membrane interactions

Introduction

Apolipophorin III (apoLp-III) is an abundant apolipoprotein found in the hemolymph of insects. The protein aids in the transport of diacylglycerol (DG), the transport form of neutral

*to whom correspondence should be addressed: eprenner@ucalgary.ca, Tel: 1-(403)-220-7632.

lipids in certain insects specialized in long distance flight [1]. The protein is made of segments of amphipathic α-helices, the structural element responsible for lipid interaction [2]. Derived from triacylglycerol (TG) stores in the fat body, a liver and adipose tissue analog, DG is transferred to circulating lipoproteins at fat body binding sites. Subsequently, up to 16 apoLp-III molecules associate with the lipoprotein surface to compensate for the increase in hydrophobicity and subsequent packing defects [3,4]. ApoLp-III has been used as a valuable model protein to gain insight in the structure and function of exchangeable apolipoproteins [5]. X-ray and NMR structures are available for apoLp-III in the lipid-free state from *Locusta migratoria* and *Manduca sexta* [6–8]. ApoLp-III is a 5-helix bundle protein, burying most of the hydrophobic residues. The polar faces of the amphipathic a-helices are directed outwards, ensuring solubility in an aqueous environment. The protein shows a strong resemblance with vertebrate apolipoproteins apoA-I and apoE (see reviews by [9–11]). Similar to human apolipoproteins, apoLp-III forms discoidal complexes when added to phospholipid liposomes [12–16]. A large protein conformational change accommodates lipid binding, and helix-helix interactions are replaced by helix-lipid interactions [14,17]. In the resulting lipid-protein complexes, termed nanodiscs, the apolipoprotein is wrapped around the periphery as an extended α-helix, covering the otherwise exposed acyl chains on the disc edge [18,19]. Similar models have been proposed for apoE and apoA-I [10,20–23]. The relatively small size of apoLp-III (164 amino acid residues), its monomeric state in solution, and availability of high-resolution structures makes it an attractive model protein to investigate the molecular details of lipid binding interaction [5].

Zwitterionic phosphatidylcholine (PC) and sphingomyelin (SM) are the main lipids of mammalian cell membranes such as erythrocytes and platelets [3,24]. In general, many mammalian membranes show an asymmetric distribution of lipid species and PC and SM are preferentially located on the outer membrane leaflet. Moreover, they are integral components of the monolayer that coats lipoprotein classes and subclasses [25]. The core of these lipoproteins is formed by cholesterol, cholesterol esters and TG. Preferential interactions of apolipoprotein with PC over SM have been reported for low density lipoprotein (LDL) [25]. Moreover, we recently showed that the actual ratio of SM to PC plays a role in modulating membrane packing and certain ratios may enhance the formation of surface defects, which in turn provide apolipoprotein binding sites. It was reported recently that PC incorporated into a SM matrix induced significant non-ideal packing and different ratios of sphingomyelin affect the domain size [26]. Multiple factors such as charge-charge interactions, membrane curvature strain and hydrophobic mismatches between the peptide and lipids play a role in ligand binding to membranes. These factors are known to cause membrane perturbation resulting in bilayer defects, phase separations or membrane thinning that could even lead to pore formation [27]. Studies with apoLp-III have indicated the importance of packing defects in the bilayer surface that enhance the binding of apoLp-III [3]. In the present study, we investigated the interactions of *L. migratoria* apoLp-III with lipid systems of varying molar ratios of PC and SM. Differential Scanning Calorimetry (DSC) was used as a non-perturbing thermodynamic technique to investigate the thermotropic phase behaviour of model lipids [28]. Moreover, changes of lipid phase characteristics were used to monitor the membrane interactions of apoLp-III from and the impact of the apolipoprotein binding on the biomimetic liposomes.

Materials and Methods

Materials

DMPC and SM (Egg, Chicken) were purchased from Avanti Polar Lipids (Alabaster, Alabama). ApoLp-III from *L. migratoria* was expressed in *Escherichia coli* BL21 cells. ApoLp-III expression was induced with IPTG and the protein purified by gel filtration chromatography and HPLC as described in detail previously [29]. Sodium phosphate, sodium

phosphate monobasic, sodium choloride and disodium ethylenediamine tetracetate were purchased from Fisher Scientific (Ottawa, Ontario).Liposome preparation: The liposomes were composed of pure egg SM, DMPC and different mixtures thereof in steps of 10 mole percent. DMPC and SM were weighed out using a Sartorius MC5 (Göttingen, Germany) microscale and dissolved in chloroform-methanol (2:1 v/v) solution. Aliquot amounts of SM and DMPC stock solutions were added to produce the desired lipid ratio. The lipids were dissolved by gentle vortexing and brief sonication in a water bath (Fisher Scientific FS100H, Ottawa Ontario). The solution was dried under a stream of argon gas and placed in a vacuum (100mm Hg) for six hours to evaporate residual solvent traces. Subsequently Multilamellar Vesicles (MLVs) were prepared by rehydrating the lipid film in PBS (Phosphate Buffer Saline; 100 mM sodium phosphate, 150 mM NaCl, 10mM EDTA, pH 7.2) to a lipid concentration of 1 mg/mL for 1 hour with periods of vortexing and brief sonication at 55°C. The hydration was done using a heating block (Fisher Scientific Isotemp 145D Ottawa, Ontario) at 10 degrees above the Tm of the lipid (DMPC 34 °C and SM 54 °C) The lipid mixtures were rehydrated at the same temperature as pure SM.

ApoLp-III solution

ApoLp-III was dissolved in PBS to prepare a protein stock solution of 10 mg/mL. The apoLp-III stock was centrifuged (Thermo IEC Micromax, Fisher, Ottawa, Ontario) at 10,000 rpm for 7 minutes to remove any undissolved protein. The final protein concentration was determined spectroscopically by using the absorbance at 280 nm of the two tryptophan residues that reside in apoLp-III (A_{280} of 0.626 = 1 mg/mL).

Apolipoprotein addition to liposomes

The liposomes were prepared as described above. Upon rehydration the vesicles were redissolved in PBS. Appropriate amounts of apoLp-III dissolved in PBS buffer were added to make a 30:1 lipid to protein ratio (1 mg/mL solution of lipid). Rehydration was done at 10 °C above the Tm of the lipid with several cycles of rigorous vortexing.

Lipid-apolipoprotein mixtures (Codissolved)

Stock solution of apoLp-III (10mg/mL), DMPC and SM (1 mg/mL) were prepared with ethanol at the selected lipid and protein ratio (30:1). The samples were then vortexed and dried under a stream of argon. The samples were further dried in a vacuum oven (100 mm Hg) for 6 hours.

DSC

Differential scanning calorimetry measurements were performed with a MicroCal VP-DSC MC-2 High Sensitivity instrument (Microcal, Northampton Massachusetts) operating at a heating or cooling rate of 10°C/hr between 5 and 55 °C. The scans were recorded in the presence and in the absence of apoLp-III using PBS as a reference. All samples were degassed by vacuum prior to use. Five scans were recorded for each vesicle preparation and the final scan was used for data analysis by subtracting the buffer prior to baseline correction using the Microcal Origin (Microcal, 7.0) software to determine the $T_{1/2}$ and Tm. Calorimetric enthalpies (ΔH_{cal}) were calculated by integrating the peak areas.

Results

MLVs are closed spherical structures that are composed of a number of concentric bilayer sheets in aqueous solution and exhibit a strong cooperative and reversible phase transition at the Tm [30]. Upon rehydration of SM and DMPC in buffer, MLVs are formed [30,31]. As discussed in detail previously, rehydrated dispersions of pure DMPC when not extensively annealed at low temperatures exhibit two endothermic events [32]. There is a less energetic

pre-transition near 14°C and a more energetic main transition near 24°C. Figure 1 illustrates DSC scans for PC, SM and mixtures. The first smaller endothermic event arises from the conversion of the L'_β to the P'_β phase and this temperature range is shown in the insert of Figure 1. The main endothermic event is the chain-melting phase and signifies the transition from the P'_β to the L_α phase. The midpoint of this transition is called the T_m and in a pure lipid the peak is symmetrical as seen with DMPC [30]. Fully hydrated egg sphingomyelin exhibited only a single asymmetric reversible phase transition at about 38.5°C, but also up to 40.5°C in other DSC studies [33]. This endotherm represents the gel to liquid crystalline phase transition for pure sphingomyelin but no pre-transition is observed. However the endotherm is considerably broader (larger $T_{1/2}$) as seen in the increased temperature range of the transition compared to DMPC. This is due to the heterogeneous acyl chain composition of egg sphingomyelin in this extract. DSC thermographs of pure DMPC, egg SM and binary mixtures clearly exhibit trends as a function of lipid composition. The pre-transition peak (Figure 1 insert) shifted to lower temperatures with increasing amounts of SM of up to 20%. In addition to the progressive shift from 11°C for pure PC to ~8°C for 20% SM, the pre-transition peak became smaller and was not detectable at SM concentrations ≥30%. Analysis of the main transition peak upon addition of SM in 10% increments exhibited a proportional increase in Tm by about 1.5°C as shown in Figure 2. The peak broadness defines the temperature range from the onset of the main transition to its completion and is commonly described by $T_{1/2}$ (peak width at half height). The DMPC peak is sharp and cooperative as expected for a synthetic, well-defined lipid and its Tm and $T_{1/2}$ values correspond to previously published values [34]. The addition of SM resulted in increased $T_{1/2}$ (broadness) of the endotherms. The observed asymmetry could be partly due to the fact that egg SM is highly enriched in C16:0 (84%) but does contain other acyl chains as well. The shape of the various peaks indicates the existence of multiple sub-peaks, which will be addressed later. The different lipid mixtures have been grouped based on their $T_{1/2}$ value (shown in legend of Figure 3). Group 1 is comprised of pure PC or low % SM (0–20% SM) and showed the lowest $T_{1/2}$ of about 1°C (white bars in Figure 3). The high % SM liposomes (90–100 %SM) and the 30% SM ratio are averaged into group 2 and show approximately a two-fold increase over group 1 ($T_{1/2}$ ~2.33). Lipid mixtures with the highest $T_{1/2}$ were observed for group 3 that consist of 40–80% SM. These mid range ratios show a significantly larger $T_{1/2}$ (~3.5°C) indicating a less ideal lipid packing. A more or less progressive increase in $T_{1/2}$ was observed up to 80% SM when groups 1–3 are compared. The 80% SM sample in group 3 displayed the broadest peak and is more symmetric compared to other peaks indicating a system with significant lipid packing problems potentially resulting in significant surface defects.

Similar to the $T_{1/2}$ values, enthalpies were averaged into three groups (Figure 4 white bars). Group 1 had the largest enthalpy (~4.7kcal/mol) and generally consisted of low or high SM ratios with the exception of 60% SM. This included pure DMPC with an enthalpy of 5.3 kcal/mol, which is close to a reported value of 5.9 kcal/mol [35]. However some biomimetic mixtures yielded noticeably lower enthalpies. These have been separated into two groups (group 2 and 3). With an average enthalpy of approximately 3.9 kcal/mol, group 2 was an average of ratios across the entire range that were 30% SM apart (10, 40, 70 % SM). Group 3 had a considerably larger deviation from either group with an average enthalpy of 2.81 kcal/mol indicating packing problems or even localized demixing.

Cooling scans mixtures containing different PCs have been shown to accentuate the different phase transitions seen in the liposome mixtures [35]. Cooling scans indicated the presence of two separate peaks which could be visualized for 60% SM in group 1 (data not shown). The two overlapping peaks showed maxima ~5°C apart indicating a peak dominated by DMPC at lower temperatures and one dominated by SM at the higher temperature.

Interaction of ApoLp-III with DMPC and SM

Addition of apoLp-III in a 30:1 lipid to protein molar ratio allows for the monitoring of protein-membrane interactions. This resulted in a large high temperature shoulder above the Tm, most visible in pure DMPC and low ratios of SM. For 100% DMPC, the pre-transition and much of the original DMPC L_α transition were still visible in the thermograph in addition to the high shoulder (Figure 5, endotherm 1). Since the pre-transition is sensitive to the presence of impurities [24], this indicated the presence of protein rich and protein poor membrane domains. The main endotherm was composed of two peaks, a sharp and narrow peak centered around 24°C (protein-poor), and a broader endotherm at 26°C (protein-rich). This directly correlates with results reported by [32] for *M. sexta* apoLp-III. This de-mixing effect suggests that a considerable amount of the DMPC is either very weakly or not interacting with apoLp-III. This is also supported by the occurrence of the pre-transition peak and is used as an indicator of lipid purity [36].

Liposomes high in DMPC content (≥ 80 % in Figure 5) interacted with the apolipoprotein in a similar manner as pure DMPC, exhibiting a well-defined sharp peak. Increased SM concentrations were accompanied by an increased transition broadness, which also indicated the presence of the two lipid components. Again, these are assigned to be a lipid dominated component (lower temperature) and a lipid-protein dominated component (higher temperature, [37]). The thermograms retained a strong resemblance to the apolipoprotein-free DMPC lipid blank (Figure 1 and Figure 4) and peak fittings showed larger $T_{1/2}$ values for SM as discussed later.

The prominence of the DMPC peak decreased with increasing SM concentrations, suggesting a disappearance of DMPC enriched domains. Increasing the SM content potentially resulted in more packing defects. This would have a positive effect on the apoLp-III interaction, resulting in a diminished resolution of protein rich and protein poor populations. At 80% SM the transition peaks were poorly resolved, as peak fitting analysis was needed to define the SM and PC peaks (Figure 6). Based on curve fitting analysis it seems that apoLp-III preferentially interacts with SM in the liposome leaving more free DMPC domains that are not interacting with SM nor with apoLp-III, resulting in separation [37]. This was proposed since the addition of apoLp-III to lipid resulted in an improved separation of the two transition components and a more visible DMPC peak. This is presumably due to the protein's preferential interaction with SM resulting in a reduced SM-PC interaction allowing the PC peak to become more resolved. The observed separation of the transition indicated at least a partial demixing between the two lipid species, resulting in two well defined peaks.

In the presence of apoLp-III, SM displayed a considerably broader endotherm with an increased ΔTm of 2°C compared to pure SM. Unlike DMPC, one transition was observed and due to the broadness of the peak, no protein-rich or poor regions were identified without peak fitting. The transition retained the general shape of the SM transition seen in the lipid blank, with the exception of a broader endotherm with a lower enthalpy. The $T_{1/2}$ value is similar to some of the PC/SM mixtures indicating a similar affinity (Figure 3).

The addition of apoLp-III resulted in an increase of Tm of ~2°C for all mixtures in a linear relationship at higher temperatures compared to the lipid mixture trend line (Figure 2, square points and small dashed line). The different slope of the apolipoprotein addition data resulted from the lower SM mixtures, whereby the Tm of the PC component is the highest point but not the midpoint of these transitions. If midpoint data were considered, the apolipoprotein addition trend line would be closer to the codissolved samples (see below). Comparing the lipid blank and apoLp-III addition, the 40% SM samples strongly deviated from the other samples, indicating an important impact of lipid composition on apolipoprotein interaction.

In addition to an increase in Tm values, a similar trend was observed for $T_{1/2}$ values as all lipid-protein mixtures displayed a broader endotherm with apoLp-III, except for pure DMPC (Figure 3). The $T_{1/2}$ values for low concentrations of SM in the presence of apoLp-III do not accurately describe the effect of the protein since $T_{1/2}$ values are calculated at half height. The taller peaks of the transition of endotherms 1, 2 and 3 (the DMPC domains) do not include the broadening of the peak due to the occurrence of peak shoulders at the base of the transition. Hence $T_{1/2}$ cannot be used as an adequate measure of the effect of the protein on liposomes in these cases. For clarity, scans for every 20% SM increment were plotted in Figure 5, but all data points were included in the trend summary of Figure 2–Figure 4 Liposomes composed of 0–30% SM excluding 20% SM (group 4 in Figure 3) showed a significantly lower $T_{1/2}$ value at 1.75°C compared to other ratios in groups 5 and 6. These values are closer to group 1 indicating minimal deviations from the PC phase transition. Group 5 had a substantial increase in $T_{1/2}$ (~8.1°C) and represents a broad range of liposomes (20, 40, 50 and 90% SM). The average $T_{1/2}$ increased about 4.5 times for group 5 and over 5 times for group 6. The increase in broadness indicates a strong disturbance of the cooperativity of the transition. The difference between group 5 and 6 is about 1.5°C and proposes a greater degree of demixing for the higher SM % ratios (60–80 and 100% SM). The $T_{1/2}$ with apoLp-III increased, reaching its maximum value at 60% SM (group 6, grey bars). The largest changes in $T_{1/2}$ were seen for the ratios >30% with the exception of 20%, which may implicate this concentration in increased packing defects. Despite the initially discussed limitations, $T_{1/2}$ value remains a useful indicator for liposomes with a SM content of >30%.

Immediately evident from Figure 4, the enthalpy was consistently lower for the protein bound systems (grey bars versus white bars). The variation between the enthalpy of the apoLp-III samples was smaller than for the lipid blanks as the average between groups 4–6 varies by less than 1 kcal/mol. Group 4 represents lower % SM with the exception of 80% SM and has the highest enthalpy for the apoLp-III addition at 3.1 kcal/mol. Group 5 is the average of the 40 and 70% SM ratios and yields a slightly lower enthalpy of 2.75 kcal/mol, which is very similar to group 3 of the lipid blanks. Group 6 contains both the pure DMPC, high SM% and mid range (50, 60% SM) and had the lowest average enthalpy for the apoLp-III addition at 2.45 kcal/mol. The enthalpy did not follow any direct trends with increasing SM concentrations, suggesting localized demixing at certain ratios.

The cooling scans showed similar results, namely an increase in the Tm and a large increase in the $T_{1/2}$, however with a nosier baseline. The presence of apoLp-III increased the width of the already broad endotherm of the gel to liquid crystalline transition (data not shown). The cooling scans were effective in increasing the resolution of the two peaks in the main transition that were faintly observed in the heating scan (especially for the 60% SM sample). When the apolipoprotein was added to the liposomes five scans were necessary for some samples to reach equilibrium which means that consecutive scans would overlay perfectly and further scanning would not change the thermodynamic parameters. Such differences between scans may be due to the fact that MLVs are composed of multiple bilayers. Thus when the apolipoprotein is added to the buffer sequential interactions with the various lamellae may occur before an equilibrium distribution is observed. Consequently, in the paragraphs below data for co-dissolved samples were investigated. Dried films containing lipids and apoprotein are hydrated to optimize the interaction of the apoprotein with the entire lipid matrix. Since the maximum interaction is facilitated no changes upon rescanning are expected.

Codissolved lipid-apolipoprotein samples

The thermograms recorded under these conditions equilibrated quickly between scans as opposed to the apoLp-III addition (Figure 7). Nevertheless, these samples exhibited the same trends as observed for apoLp-III addition to liposomes. The Tm and $T_{1/2}$ increased with rising

SM concentrations with the largest $T_{1/2}$ observed at 60% SM, and the enthalpy was consistently lower in the presence of apolipoprotein (Figure 2–Figure 4). The observed trends were similar, but the absolute extent of the interactions was more pronounced for co-dissolved samples. This is particularly obvious for DMPC, which only exhibits one broader peak as opposed to the obvious protein rich and protein poor domains (Figure 5 and Figure 7 endotherm 1). The codissolved endotherms were broader, displayed a lower enthalpy and shifted Tm compared to the lipid blanks. The Tm, $T_{1/2}$ and enthalpy trends shown in Figure 2–Figure 4 respectively follow the apolipoprotein addition trials. Compared to both the lipid blank and apoLp-III addition trials, the phase transition had an increased Tm with an upward shift of the trend line (Figure 2). The codissolved trend line for Tm runs almost parallel to the lipid matrix trend line and above the apolipoprotein addition trend line indicating that the codissoved trials elicited a more pronounced interaction (figure 2 triangles and dashed line).

The $T_{1/2}$ of the codissolved samples in Figure 3 show more consistent values than the apoLp-III addition trials. Group 7 consists of the majority of the codissolved liposomes from 0–80% SM with the exception of 10, 50 and 70% SM. The $T_{1/2}$ was more than double than any of the lipid blank samples. 30% SM (group 7) had the narrowest distribution compared to other codissolved liposomes indicating a stronger lipid matrix effect in this mixture. Group 8 has an average $T_{1/2}$ close to group 5 suggesting a similar degree of broadening induced by apoLp-III in either group. Values between 50 and 80 % SM excluding 70% (group 9) showed the largest $T_{1/2}$ for the codissolved at 9°C, which is approximately 0.5°C lower than observed for group 6. This represents a similar extent of interaction between the two groups possible due to localized demixing. When this data is compared to the apolipoprotein addition values, the codissolved samples are narrower for the majority of the liposomes (group 8 and 9 compared to group 6 and 7). This indicates that lipid packing problems affect the interaction of the apolipoprotein in the apolipoprotein addition experiments, whereas the simultaneous hydration of lipids and proteins resulted in comparably narrower and homogenous peaks.

Enthalpy values for the codissolved samples were much lower than lipid mixtures and lower than the apolipoprotein addition data. Group 7 consists of the even ratios and 30% SM except 100%SM. The average enthalpy value (2.4 kcal/mol) is almost identical to group 6 indicating a similar effect from apoLp-III. The average enthalpy decreased by about 0.5 kcal/mol for group 8 (ratios 10, 50, 70 and 100 %SM). This group has the lowest enthalpy with the exception of 90% SM codissolved (group 9). 90% SM has an average enthalpy of just over 1 kcal/mol, which is nearly half of the next smallest enthalpy (group 8). The conspicuous lower values at 90% SM indicate stronger protein interactions potentially facilitated by lipid packing and surface defects.

Comparing the codissolved thermogram (Figure 7) to the apolipoprotein addition (Figure 5), there is significantly less demixing present within the liposomes. The transitions appear as one single peak and not as two components of different lipids. When the apolipoprotein is added to MLVs, the protein seems to interact stronger with the SM fraction of the liposomes, thereby diminishing SM-PC interactions as well as the SM enriched domains. This seems to result in more PC-enriched domains that lead to two discernible peaks in the mixtures. This was proposed based on the trends observed from the Gaussian fittings explained later. Endotherm 4 in Figure 7 represents 60% SM and shows the greatest $T_{1/2}$ value and the highest interaction with apoLp-III. Further increase in SM concentration resulted in $T_{1/2}$ values between 8.5 and 10°C with the persistence of the two component transition seen up to 80% SM (Figure 7 endotherms 2–5). The $T_{1/2}$ data also corresponds to DSC findings by [24] who demonstrated that SM addition to POPC bilayers induced peak broadening.

Variations due to lipid composition also indicate a role of surface defects within the lipid mixtures, which provide increased binding sites for apoLp-III. When the codissolved samples

are compared to the lipid matrices, much less low temperature peak tailing and overall broader peaks with a higher transition temperature were observed. This indicated a strong interaction of the protein that facilitates the mixing of the lipid matrix. The overall slight upshift in Tm indicated a stabilization of the lipid gel phase in the presence of protein.

Since several peaks from the protein addition trials indicated multi-component peaks, we performed Gaussian 2 Fitting analysis (Origin 7.5) on the thermotropic data as shown in Figure 6. In figure 6A a sample of the curve fitting and the parameters generated are shown. The ratio of 80% SM with apoLp-III shows a 2 peak fitted analysis that has equal contribution from both a presumably PC-enriched peak at the lower Tm and a SM enriched fraction exhibiting the higher phase transition temperature. ApoLp-III caused a broadening and reduction in total enthalpy of all liposomes. Even in higher percentage SM liposomes a significant PC dominated peak is observed, indicating a preferential interaction of apoLp-III with SM. The Tm trends for the two peaks are shown in 7B. The trend lines are not parallel with peak 2 (dashed SM) having a larger slope indicating a greater shift in the melting temperature. This suggested that there is a stronger interaction between apoLp-III and SM than with DMPC indicative by the larger shift in Tm. The $T_{1/2}$ trends for selected mixtures are show in Figure 6C. These points were selected from mixtures that showed the largest deviation in the $T_{1/2}$ data displayed in Figure 3. Although there is a large deviation between the maximum and minimum values for two experiments with 70% SM, the other data showed a trend where there is a clear separation between the DMPC and the SM peak. The $T_{1/2}$ is larger for the SM peak in the ratios from 40–70% SM. In addition, the enthalpy fittings shown in Figure 6D from the same samples revealed a lower enthalpy for the SM component compared to PC. At 80% SM a slight deviation from the trend was observed, although only two data sets were used in the fitting analysis and the significance of this enthalpy is not known. In general, the Tm and enthalpy fits support the stronger interaction of the apoprotein with SM resulting in broader peaks with reduced enthalpy.

Discussion

The structural resemblance of apoLp-III with human apolipoproteins implies a common mechanism for lipid binding interaction. ApoLp-III predominantly binds to lipoprotein surfaces highly enriched in DG in vivo. Human and insect lipoproteins are similar is size and density, and both contain integral apolipoproteins, i.e. apoLp-I and -II in lipophorin and apoB in LDL. Lipid compositions are quite different, although phospholipids are abundant in both lipoproteins and may be the main lipid component to which apolipoproteins bind [38]. Insect lipoproteins contain DG, and phospholipids, including sphingomyelin, but TG and cholesterol esters are vitually absent [3,39]. On the other hand, DG is noticeably absent from vertebrate apolipoproteins [40]. While both invertebrate and vertebrate systems differ in several aspects, there are important similarities, in particular the resemblance in apolipoprotein structure and the interaction with PC vesicles resulting in the formation of similarly shaped nanodiscs [5, 16,41]. Sphingomyelin is an important membrane component affecting its integrity and may require apolipoprotein binding interaction with lipoprotein surfaces. ApoLp-III was used as a model apolipoprotein to gain insight in the effect of SM on lipid packing and apolipoprotein binding interaction. The calorimetric experiments performed on the DMPC and SM vesicles with apoLp-III provide quantitative and qualitative information about their interactions. DSC data offered information about the phase transition(s) of the liposomes upon interaction with the apolipoprotein by analyzing thermotropic data such as the midpoint of the phase transition, Tm, the overall cooperativity of the peak, $T_{1/2}$ and the peak area, which correspond to the enthalpy of the transition.

Some of these investigated lipid mixtures mimic the composition of human lipoproteins, which consists of 70% PC and 30% SM in LDL and 15% PC and 85% SM in HDL [26]. All liposomes

exhibited characteristic thermographs. The sharp main transition at 24°C of pure DMPC became increasingly broader with the addition of SM (until 80% SM). In addition, the Tm increased with each SM addition, eventually reaching values near the SM transition temperature of 39°C. The pre-transition at 12°C observed for pure DMPC is a characteristic feature of the DMPC endotherm. The presence of small percentages of SM in the DMPC bilayers resulted in strong reductions of the pre-transition. This is due to the sensitivity of the PC bilayer to the presence of other lipid species such as SM which usually abolishes the pre-transition with a high concentration of apoLp-III [32]. The persistence of the pre-transition even at 20% SM indicates that pure DMPC domains still exist and have not yet been perturbed by interaction of the protein [32]. At 20% SM the pre-transition had slightly shifted towards the low temperature side of the transition and was significantly attenuated in terms of the enthalpy and by 40% SM the pre-transition was not visible. This indicates that increasing SM concentrations reduce the amount of pure DMPC domains that are available for this pre-transition. As mentioned in the results, there appeared to be two peaks overlapping in some of the endotherms for some of the PC/SM mixtures seen in Figure 1. In cooling scans these peaks became more defined suggesting that liposomes do not undergo a one cooperative transition but consists of a predominately DMPC and SM peak within the endotherm during transition. The effect of two overlapping endotherms in lipid mixtures has been seen with binary mixtures of DMPC and DMPG [32].

The main transition is simplified as the gel to fluid transition where crystalline lateral packing is converted to a form the less ordered liquid- crystalline phase [42]. In more recent work this change in the lipid state was proposed to lead to the formation of domains, which are accompanied by the decrease in the order of the chains. These domains represent a localization of a lipid species within a bilayer [43]. Such domains have been described as “floating” in a membrane” and were proposed to be enriched in SM. [37]. In a PC matrix with the addition of cholesterol and SM immiscibility can form leading to domain formation [37]. The immiscibility can also form surface defects in the matrix and such domains may thus form sites for apoLp-III interaction.

Upon comparison of the thermographs of the various DMPC and SM vesicles it is apparent that apoLp-III preferred a binding interaction with SM compared to DMPC (Figure 5). The lipid mixtures, particularly 40% DMPC and 60% SM displayed the greatest binding affinity and interaction with apoLp-III. In the thermograph for DMPC the sharp component comprising the transition from the gel to liquid crystalline phase represent the DMPC domains, which are not interacting with the protein. However when apoLp-III binds, this peak becomes slightly attenuated indicating less free DMPC domains. The broad component of the thermograph is observed at a higher temperature than the Tm of the lipid blank due to lipid domains that are perturbed by the apoLp-III interaction. This is supported further by the effect of apoLp-III interaction with the pre-transition peak of the lipid. In previous studies, it was found that at all lipid to protein ratios a pre-transition remained visible along with the main transition [32]. However the enthalpy of the pre-transition decreased with a reduction in the lipid to protein ratio. This correlates with our findings as more lipids interact with apoLp-III, the fewer free lipids show the pre-transition or the pure gel to L_α phase.

Addition of apoLp-III did not indicate a strong affinity for pure DMPC. The overall main transition showed little changes in the Tm, $T_{1/2}$ and enthalpy. However the codissolved method of preparation forces the protein to interact maximally with the lipids and resulted in a considerable change in Tm, $T_{1/2}$ and enthalpy. This demonstrates that the affinity for DMPC is quite low with apoLp-III upon comparison with the maximal interaction observed with the codissolved method. The similarities between the thermotropic values for samples with and without apoLp-III indicate that there was not a significant alteration in the chain packing of the hydrocarbons during the phase transition. However the large shoulder evident in figure 5

of the pure DMPC peak shows that there is interaction between the liquid crystalline state of the lipids and the protein [32]. The gel phase of the transition did not show any perturbation or changes in the endotherm. As mentioned earlier the liquid crystalline state has considerably more disorder in the lipid acyl chains and adds surface defects to the bilayer. These defects can possibly act as binding sites for apoLp-III allowing for greater interaction. In order to have a stronger interaction visualized by a larger shift in the Tm and a larger $T_{1/2}$ there must be a more significant disruption in the lipid packing to induce surface defects. The shift in Tm upon binding became less pronounced with vesicles that were predominately SM or DMPC indicating the importance of decreased membrane stability due to lipid heterogeneity in apoLp-III binding. The largest ΔTm was observed for mixtures containing 40%–60% DMPC and the increase in $T_{1/2}$ indicates that large populations of lipids are interacting with apoLp-III as fewer lipids remain at the original Tm. However, biological lipid mixtures and biomimetic vesicles with low percentages of DMPC have asymmetric traces and the Tm may not represent the midpoint of the phase transition especially with heterogeneous liposomes with visible domains of DMPC and or SM [44].

Data from the protein addition sets indicated multi-component peaks contributing to the transition (for example thermogram 5 in Figure 5). Gaussian Fittings were performed to assess differential interaction of the apolipoprotein with PC or SM. Figure 6B shows a larger shift in the Tm data for SM, which indicates an increased interaction with the SM component. Figure 6C supports the larger shifts seen in 6B with a greater increase in the $T_{1/2}$ for the SM component. This can be attributed to packing defects that are caused by the largely heterogeneous mixtures of DMPC and SM. Such packing problems are illustrated in Figure 8. Ideal packing of homogeneous samples of smaller circles (PC) in panel A and larger circles (SM) are shown in panel B. The smaller PC is able to accommodate larger SMs better (panel C) as compared to a smaller PC in a SM matrix (panel D). X-ray diffraction studies on liposomes composed of binary mixtures of SM and PC also indicated that PC can be accommodated in a low concentration in a SM matrix without disturbing the hydrocarbon chain packing [24]. In addition, at SM values above 50% the formation of distinct SM domains in these mixtures was observed that would grow in size with an increase in SM concentration. SM enriched samples in the protein addition series indicated a stronger interaction with SM (see the emergence of a lower temperature peak in Figure 5) which was supported by the above mentioned peak fitting. Moreover, the lower enthalpy observed for the SM component (panel 7D) also suggests that apoLp-III preferentially interacts with SM. Both effects, preferential interaction with SM or packing defects at the edge of larger SM domains as well as packing defects on a smaller scale as illustrated in Figure 8, could contribute to the enhanced interaction with SM. A comparable preference was shown by liposome to nanodisc transformation analysis with apoA-I, showing increased nanodisc formation rates at higher ratios of SM to PC in liposomes [45].

The interaction of proteins with lipids has been characterized by three different types of binding models. These have been referred to as Type 1, 2 and 3 models based on their effects on phospholipid gel to liquid-crystalline phase transitions [30]. ApoLp-III has similarities to the Type 1 proteins, which interact with membrane lipids via polar and or electrostatic forces at the bilayer surface without significant penetration of the hydrophobic core of the bilayers, and their permeability is not affected [32,46]. Type 1 interactions are known to show a modest increase in the Tm and $T_{1/2}$ as observed in our data. Moreover, the enthalpy change is proportional to the amount of protein added which also correlates well with our data.

In many mammalian membranes PC and SM are the predominant phospholipids but are found at varying ratios (for a detailed discussion see [26]). Fukuda et al 2007 [45] found that heterogeneous interfaces facilitate the insertion of apoA-I, similar to the results seen for apoLp-III. ApoA-I interacts with DMPC rich domains at the Tm due to pores formed in the bilayer at the boundary phase between the gel and liquid crystalline [47]. A relatively high rate of

interaction between apoA-I and DMPC matrix is attributed to a large percentage of boundary lipids, which cause lattice defects in the L_d phase [12]. The defects can be attributed to the increased rate of flip-flop found at the phase transition. Further evidence for packing defects have been observed for sonicated egg phosphatidylcholine, which showed that heterogeneity of fatty acid tails resulted in packing defects which may influence the L_α state interaction with apoA-I [42]. Phospholipids are known to flip flop within bilayers from the outer leaflet to the inner leaflet or vice versa. At the Tm, packing defects that can induce rapid transbilayer lipid diffusion are likely to occur when phases coexist [48]. Furthermore, membrane spanning proteins have been shown to induce membrane perturbations in bilayers using fluorescence and phospholipid analogs. Surface defects influences the phospholipids flip-flop rate and are involved in many physiological activities such as stimulating ion permeability in the bilayer [45]. The phospholipid phase transition is described as occurring in clusters with approximately 100 phospholipids. The size of these clusters has direct correlation with the cooperativity of the phase transition and is related to the size and amount of surface defects [45]. It is proposed that during the main transition from the gel to liquid crystalline phase that with high amounts of SM in a PC matrix the gel converts to a L_d phase (liquid disordered phase). The L_d phase has a higher predisposition to form packing defects, upon which apoLp-III may be able to bind. ApoLp-III inserts into a lattice defect at this gel to liquid crystalline phase interface that arises in the L_d phase. The heterogeneous interface at the L_d phase enhances packing defects, which changes the local environment of the phospholipids that increases apolipoprotein binding affinity [45]. The presence of these L_d and L_o (liquid ordered) phases lead to the formation of domains upon which proteins can interact [49]. Due to the binding seen predominately at the phase transition temperature this may be due to the activation energy of the lipid-protein interaction only occurring near the Tm, which provides the maximal number of surface defects at the boundaries of the gel and liquid crystalline phases where permeability is greatest [12]. This is in support with both human apoA-I and apoA-II, which showed an increased rate of association around the T_m [42,50].

As discussed previously, the in vivo molar ratios of PC and SM in mammalian membranes vary significantly, and these differences may affect membrane function and biophysical characteristics. Thus, the presence of two different lipids induces lateral heterogeneity since molecular packing in the bilayer depends on molecular shape, size and charge of the lipids. Although SM and PC are very similar in terms of headgroup structure, the difference in the backbone can account for lipid composition dependent non-ideal packing [26]. The additional hydroxyl group and amide linked hydrocarbon chain of the SM backbone provides hydrogen bonding opportunities which may result in increased rigidity. Such a tighter packing of SM matrices over PC was also observed by fluorescence anisotropy in bilayer systems [51]. Brewster angle microscopy showed the formation of distinct lateral domains in SM-rich mixtures whereby the size increasing with the SM content [26]. At 60% SM smaller but more numerous domains were observed. Moreover, nearest neighbour recognition studies also indicated higher probability of packing and surface defects upon increased lateral heterogeneity [52], which may provide more apoLp-III interaction sites. Surface defects are most prevalent at the melting temperature of the gel and liquid crystal phase, hence binding is only observed around a small range near the phase transition temperature. Studies reported by Arnulphi et al [53,54] showed that the introduction of SM into POPC liposomes created surface defects which increased apoA-I binding [13]. These surface defects are not just limited to SM and PC liposomes, but the addition of DG has also been known to cause this effect [32]. Hence higher amounts of SM will increase the amount of surface defects in liposomes and create additional apoLp-III binding sites.

The presented data showed the broadest transition ($T_{1/2}$) at 40% DMPC and 60% SM indicating the highest affinity of apoLp-III. Thus packing defects at certain ratios (30% SM, 70–80% SM) as well as the presence of lipid domains (at higher SM concentrations) could affect the binding

of the apolipoprotein to these mixtures. Using pressure-area isotherms significant non ideal mixing as a function of lipid composition was observed which also affected lipid compressibility, surface potential and domain formation [26]. These authors reported the highest packing defects at ~30% SM and at 70–80% SM, which are the mixtures that showed conspicuous trends in the current calorimetric analysis.

In conclusion, the calorimetric studies showed the thermodynamic properties of DMPC/SM liposomes upon interaction with apoLp-III. The shift in Tm, $T_{1/2}$ and enthalpy indicated an increased apolipoprotein affinity with SM domains in binary PC/SM mixtures. The increased affinity of apoLp-III with higher ratios of SM suggests the role of surface defects, facilitating apolipoprotein binding. Moreover, the potential existence of distinct rigid SM domains may also contribute to the enhanced binding interaction [26]. The calorimetric data presented helps to elucidate the role of non ideal packing as a major factor in the interaction of apoLp-III with biomimetic PC and SM vesicles. The structural and functional similarity with other apolipoproteins makes apoLp-III a valuable protein to clarify the role of lipid packing as a function of overall lipid composition. Thus, a better understanding of its membrane interactions can be relevant for apolipoprotein membrane interaction in general and help to elucidate the mechanism of lipoprotein assembly.

Abbreviations

apoA-I, apolipoprotein
A-I, apoE apolipoprotein E
apoLp-III, apolipophorin III
DAG, diacylgycerol
ApoLp-I/II, apolipophorin I and apolipophorin II
DMPC, 1,2-dimyristoyl-sn-glycero-3-phosphocholine
DSC, differential scanning calorimetry
DLS, dynamic light scattering
HDLp, high density lipophorin
ITC, isothermal titration calorimetry
LDLp, low density lipophorin
MLV, multilamellar vesicle
PBS, phosphate buffered saline
PC, phosphatidylcholine
SM, sphingomyelin
POPC, 1-palmitoyl-2-oleoyl-sn-glycero-3-phosphocholine
SUV, small unilamellar vesicle
Tm, phase transition temperature
$T_{1/2,}$, A measure of peak broadness referring to the range between the half heights of the peak
TAG, triacylglycerol

Acknowledgments

This work was support by a NSERC discovery grant to EJP and NIH grant (R15 HL 077135) to PMMW. MC was supported by NSERC and AHFMR summer fellowships.

References

1. Ryan RO, VanderHorst DJ. Lipid transport biochemistry and role in energy production. Ann. Rev. Entomol 2000;45:233–260. [PubMed: 10761577]
2. Segrest JP, DeLoof H, Dohlman JG, Brouillette CG, Anatharamaiah GM. Amphipathic Helix Motif: Classes and Properties. Proteins 1990;8:103–117. [PubMed: 2235991]

3. Soulages JL, Wells MA. Lipophorin: the structure of an insect lipoprotein and its role in lipid transport in insects. Adv. Protein. Chem 1994;45:371–415. [PubMed: 8154373]
4. Weers PMM, Ryan RO. Apolipophorin III: a lipid-triggered molecular switch. Insect Biochem. Molec 2003;33:1249–1260.
5. Weers PMM, Ryan RO. Apolipophorin III: role model apolipoprotein. Insect. Biochem. Molec 2006;36:231–240.
6. Breiter DR, Kanost MR, Benning MM, Wesenberg G, Law JH, Wells MA, Rayment I, Holden HM. Molecular-Structure of An Apolipoprotein Determined at 2.5-A Resolution. Biochemistry 1991;30:603–608. [PubMed: 1988048]
7. Wang JJ, Sykes BD, Ryan RO. Structural Basis for the Conformational Adaptability of Apolipophorin III, a helix-bundle exchangeable apolipoprotein. Proc. Natl. Acad. Sci. U S A 2002;99:1188–1193. [PubMed: 11818551]
8. Fan D, Zheng Y, Yang D, Wang J. NMR solution structure and dynamics of an exchangeable apolipoprotein, Locusta migratoria apolipophorin III. J. Biol Chem 2003;278:21212–21220. [PubMed: 12621043]
9. Saito H, Lund-Katz S, Phillips MC. Contributions of domain structure and lipid interaction to the functionality of exchangeable human apolipoproteins. Prog. Lipid Res 2004;43:350–380. [PubMed: 15234552]
10. Hatters DM, Peters-Libeu CA, Weisgraber KH. Apolipoprotein E structure: insights into function. Trends Biochem. Sci 2006;31:445–454. [PubMed: 16820298]
11. Davidson WS, Thompson TB. The Structure of Apolipoprotein A-I in High Density Lipoproteins. J. Biol. Chem 2007;282:22249–22253. [PubMed: 17526499]
12. Pownall HJ, Massey JB, Kusserow SK, Gotto AM. Kinetics of Lipid-Protein Interactions: Interaction of Apolipoprotein A-1 from Human Plasma High Density Lipoproteins with phosphatidylcholines. Biochemistry 1978;17:1183–1188. [PubMed: 207309]
13. Surewicz WK, Epand RM, Pownall HJ, Hui SW. Human apolipoprotein A-I forms thermally stable complexes with anionic but not with zwitterionic phospholipids. J. Biol. Chem 1986;261:16191–16197. [PubMed: 3097001]
14. Wientzek M, Kay CM, Oikawa K, Ryan RO. Binding of Insect Apolipophorin III to Dimyristoylphosphatidylcholine Vesicles. J. Biol Chem 1994;269:4605–4612. [PubMed: 8308032]
15. Weers PMM, Kay CM, Oikawa K, Wientzek M, VanderHorst DJ, Ryan RO. Factors affecting the stability and conformation of Locusta migratoria apolipophorin III. Biochemistry 1994;33:3617–3624. [PubMed: 8142360]
16. Chromy BA, Arroyo E, Blanchette CD, Bench G, Benner H, Cappuccio JA, Coleman MA, Henderson PT, Hinz AK, Kuhn EA, Pesavento JB, Segelke BW, Sulchek TA, Tarasow T, Walsworth VL, Hoeprich PD. Different apolipoproteins impact nanolipoprotein particle formation. J. Am. Chem. Soc 2007;129:14348–14354. [PubMed: 17963384]
17. Raussens V, Narayanaswami V, Goormaghtigh E, Ryan RO, Ruysschaert J. Alignment of the Apolipophorin-III α-Helices in Complex with Dimyristoylphosphatidylcholine. J. Biol. Chem 1995;270:12542–12547. [PubMed: 7759500]
18. Sahoo D, Weers PMM, Ryan RO, Narayanaswami V. Lipid-triggered conformational switch of apolipophorin III helix bundle to an extended helix organization. J Mol Biol 2002;321:201–214. [PubMed: 12144779]
19. Garda HA, Arrese EL, Soulages JL. Structure of apolipophorin-III in discoidal lipoproteins. J. Biol. Chem 2002;277:19773–19782. [PubMed: 11896049]
20. Raussens V, Fisher CA, Goormaghtigh E, Ryan RO, Ruysschaert J. The low Density lipoprotein Receptor Active Conformation of Apolipoprotein E. J. Biol. Chem 1998;273:25825–25830. [PubMed: 9748256]
21. Segrest JP, Jones MK, Klon AE, Sheldahl CJ, Hellinger M, Loof HDe, Harvey SC. A detailed molecular belt model for apolipoprotein A-I in discoidal high density lipoprotein. J. Biol. Chem 1999;274:31755–31758. [PubMed: 10542194]
22. Narayanaswami V, Maiorano JN, Dhanasekaran P, Ryan RO, Phillips MC, Lund-Katz S, Davidson WS. Helix Orientation of the functional domains in apolipoprotein E in discodial heigh density lipoprotein particles. J. Biol. Chem 2004;279:14273–14279. [PubMed: 14739281]

23. Silva RA, Huang R, Morris J, Fang J, Gracheva EO, Ren G, Kontush A, Jerome WG, Rye KA, Davidson WS. Structure of apolipoprotein A-I in spherical high density lipoproteins of different sizes. Proc. Natl. Acad. Sci. U S A 2008;105:12176–12181. [PubMed: 18719128]
24. Degovics G, Latal A, Prenner E, Kriechbaum M, Lohner K. Structure and Thermotorpic Behaviour of Mixed Choline Phospholipid Model Membranes. J. Appl. Cryst 1997;30:776–780.
25. Sommer A, Prenner E, Gorges R, Stutz H, Grillhofer H, Kostner G, Paltauf G, A H. Organization of Phosphatidylcholine and Sphingomyelin the Surface Monolayer of Low Density Lipoprotein and Lipoprotein(a) as Determined by Time-resolved Fluorometry. J. Biol. Chem 1992;267:24217–24222. [PubMed: 1447171]
26. Prenner E, Honsek G, Honig D, Mobius D, Lohner K. Imaging of the domain organization in sphingomyelin and phosphatidylcholine monolayers. Chem. Phys Lipids 2007;145:106–118. [PubMed: 17188673]
27. Lohner K, Prenner E. Differential Scanning Calorimetry and X-ray diffraction studies of the specificity of the interaction of antimicrobial peptides with membrane-mimetic systems. Biochim. Biophys. Acta 1999;1462:141–156. [PubMed: 10590306]
28. Lamparski H, Lee Y, Sells T, O'Brien D. Thermotropic Properties of Model Membranes Composed of polymerizable Lipids. 1. Phosphatidylcholines containing terminal acryloyl, methacryloyl, and Sorbyl Groups. J. Am. Chem. Soc 1993;115:8096–8102.
29. Weers PMM, Wang J, VanderHorst DJ, Kay CM, Sykes BD, Ryan RO. Recombinant locust apolipophorin III: characterization and NMR spectroscopy. Biochim. Biophys. Acta 1998;1393:99–107. [PubMed: 9714761]
30. McElhaney R. The Use of Differential Scanning Calorimetry and Differential Thermal Analysis in Studies of Model and Biological Membranes. Chem.Phys. Lipids 1982;30:229–259. [PubMed: 7046969]
31. Jacobson MK, Lehman MM, Jacobsohn GM. Cell Membranes and Multilamellar Vesicles: Influence of pH on Solvent Induced Damage. Lipids 1992;27:694–700. [PubMed: 1487967]
32. Zhang Y, Lewis R, McElhaney R, Ryan RO. Calorimetric and Spectroscopic Studies of the Interaction of Manduca sexta Apolipophorin III with Zwitterionic, Anionic and, Nonionic Lipids. Biochemistry 1993;32:3942–3952. [PubMed: 8471606]
33. Maulik PR, Shipley GG. Interactions of N-Stearoyl Sphingomyelin with Cholesterol and Dipalmitoylphosphatidylcholine in Bilayer Membranes. Biophys. J 1996;70:2256–2265. [PubMed: 9172749]
34. Prenner E, Lewis R, Kondejewski L, Hodges R, McElhaney R. Differential Scanning Calorimetric Study of the effect of the antimicrobial peptide gramicidin S on the thermotropic phase behavior of phosphatidylcholine, phosphatidylethanolamine and phosphatidylglycerol lipid bilayer membranes. Biochim. Biophys. Acta 1999;1417:211–223. [PubMed: 10082797]
35. Lewis R, Mak N, McElhaney R. A differential Scanning Calorimetric Study of the Thermotropic Phase behavior of Model Membranes Composed of Phosphatidylcholines Containing Linear Saturated Fatty Acyl Chains. Biochemistry 1987;26:6118–6126. [PubMed: 3689765]
36. Biltonen RL, Lichtenberg D. The use of Differential Scanning Calorimetry as a tool to characterize liposome preparations. Chem Phys. Lipids 1993;64:129–142.
37. Epand RM. Detecting the Presence of Membrane Domains using DSC. Biophys. Chem 2007;126:197–200. [PubMed: 16730877]
38. Wang JJ, Liu H, Sykes BD, Ryan RO. Phosphorus-31 NMR study of the phospholipid moiety of lipophorin subspecies. Biochemistry 1992;31:8706–8712. [PubMed: 1390655]
39. Beenakkers AMT, VanderHors DJ, VanMarrewijk WJA. Insect lipids and lipoproteins, and their role in physiological processes. Prog. Lipid. Res 1985;24:19–67. [PubMed: 3916237]
40. Jonas, A.; Phillips, MC. Structure Lipoprotein. In: Vance, DE.; Vance, JE., editors. Biochemistry of Lipids Lipoproteins and Membranes. Amsterdam: Elsevier BV; 2008. p. 485-506.
41. VanderHorst DJ, VanHoof D, VanMarrewijk WJ, Rodenburg KW. Alternative lipid mobilization: the insect shuttle system. Mol Cell Biochem 2002;239:113–119. [PubMed: 12479576]
42. Epand RM. The Apparent Preferential Interaction of Human-Plasma High-Density Apolipoprotein A-1 with Gel State Phospholipids. Biochim. Biophys. Acta 1982;712:746–751.

43. Oliynyk V, Jäger M, Heimburg T, Buckin V, Kaatze U. Lipid membrane domain formation and alamethicin aggregation studied by Calorimetry, sound velocity measurements, and atomic force microscopy. Biophys. Chem 2008;134:168–177. [PubMed: 18342426]
44. McElhaney R. Differential Scanning Calorimetric Studies of Lipid-Protein Interactions in Model Membrane systems. Biochim. Biophys. Acta 1986;864:361–421. [PubMed: 3539194]
45. Fukuda M, Nakano M, Sriwongsitanont S, Ueno M, Kuroda Y, Tetsurou H. Spontaneous reconstitution of discoidal HDL from Sphingomyelin-containing model membranes by apoliporptein A-1. J. Lipid. Res 2007;48:882–889. [PubMed: 17224608]
46. Sahoo D, Narayanaswami V, Kay CM, Ryan RO. Fluorescence studies of exchangeable apolipoprotein-lipid interactions. Superficial association of apolipophorin III with lipoprotein surfaces. J. Biol. Chem 1998;273:1403–1408. [PubMed: 9430675]
47. Pownall HJ, Massey JB, Kusserow SK, Gotto AM. Kinetics of Lipid-Protein Interactions: Effect of Cholesterol on the Association of Human Plasma High-Density Apolipoprotein A-1 with L-α-Dimyristoylphosphatidylcholine. Biochemistry 1979;18:574–579. [PubMed: 217418]
48. John K, Schreiber S, Kubelt J, Hermann A, Muller P. Transbilayer Movement of Phospholipids at the Main Phase Transition of Lipid Membranes: Implications for Rapid Flip-Flop in Biological Membranes. Biophys. J 2002;83:3315–3323. [PubMed: 12496099]
49. Brown DA. Lipid Rafts, Detergent-Resistant Membranes, and Raft Targeting Signals. Physiology 2006;21:430–439. [PubMed: 17119156]
50. Jayaraman S, Gursky GDLO. Kinetic Stabilization and Fusion of Apolipoprotein A-2:DMPC Disks: Comparison with apoA-1 and apoC-1. Biophy J 2005;88:2907–2918.
51. Prenner E, Sommer A, Maurer N, Glatter O, Gorges R, Paltauf F, Hermetter A. Lateral Microheterogeneity of Diphenylhexatriene-Labeled Choline Phospholipids in the Erythrocyte Ghost Membrane as Determined by Time-Resolved Fluorescence Spectroscopy. J. Membr. Biol 2000;174:237–243. [PubMed: 10758177]
52. Uragami M, Dewa T, Regen IMHRS. Influence of Head Group Mismatch on the Miscibility of Phospholipids in the Physiologically-Relevant Fluid Phase: A Nearest-Neighbor Recognition Analysis. J. Am. Chem. Soc 1997;119:3797–3801.
53. Arnulphi C, Sánchez SA, Tricerri MA, Gratton E, Jonas A. Interaction of human apolipoprotein A-I with model membranes exhibiting lipid domains. Biophys. J 2005;89:285–295. [PubMed: 15849246]
54. Arnulphi C, Jin L, Tricerri MA, Jonas A. Enthalpy-driven apolipoprotein A-I and lipid bilayer interaction indicating protein penetration upon lipid binding. Biochemistry 2004;43:12258–12264. [PubMed: 15379564]

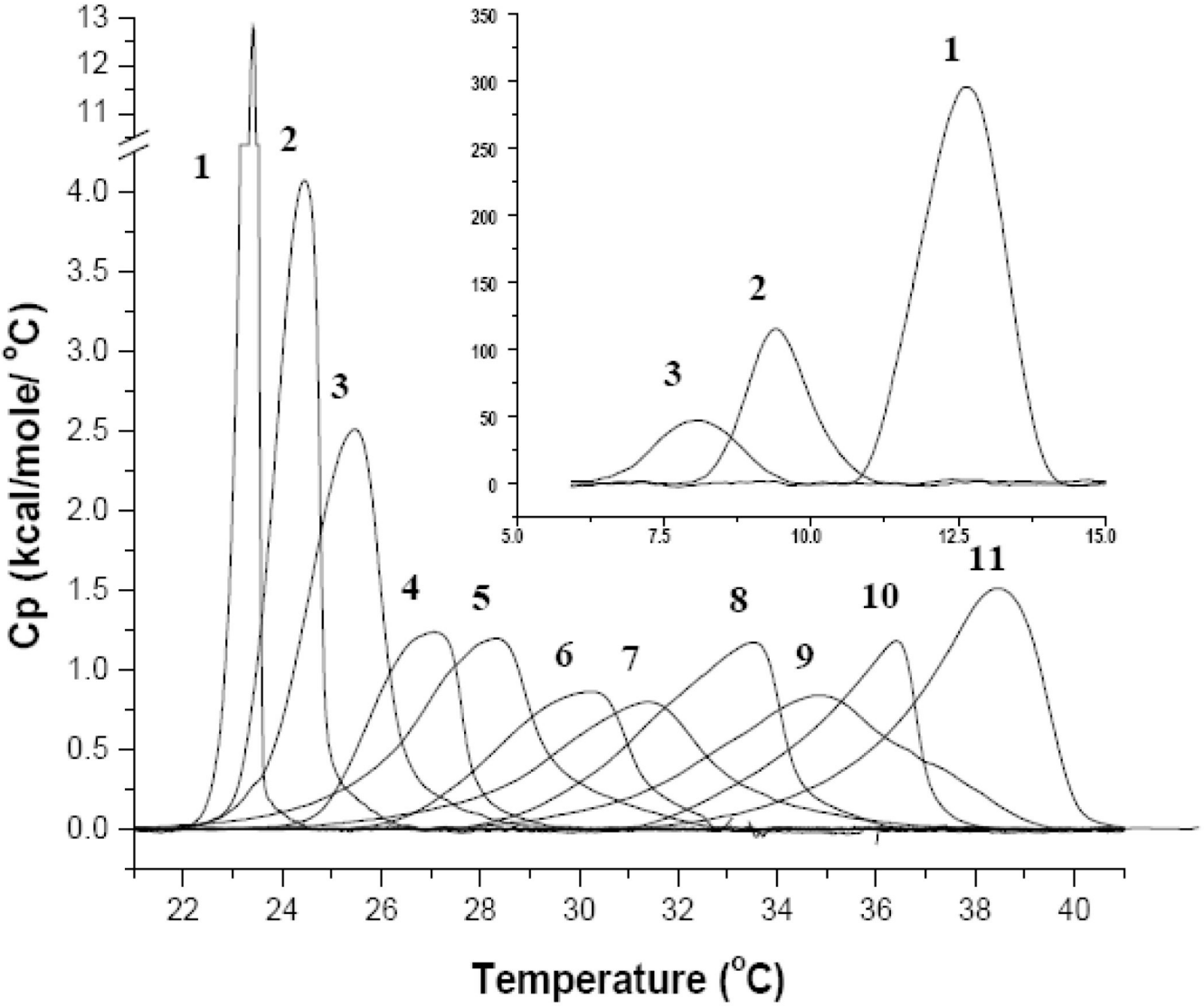

Figure 1.

DSC Heating Thermographs of DMPC/SM mixtures in MLVs (1mg/mL PBS; heating rate of 10°C/hour) 1) 100% DMPC 2) 10% SM 3) 20% SM 4) 30% SM 5) 40% SM 6) 50% SM 7) 60% SM 8) 70% SM 9) 80% SM 10) 90% SM 11) 100% SM. The insert shows the pre-transitional peak for 1), 2) and 3) from 5 −15°C.

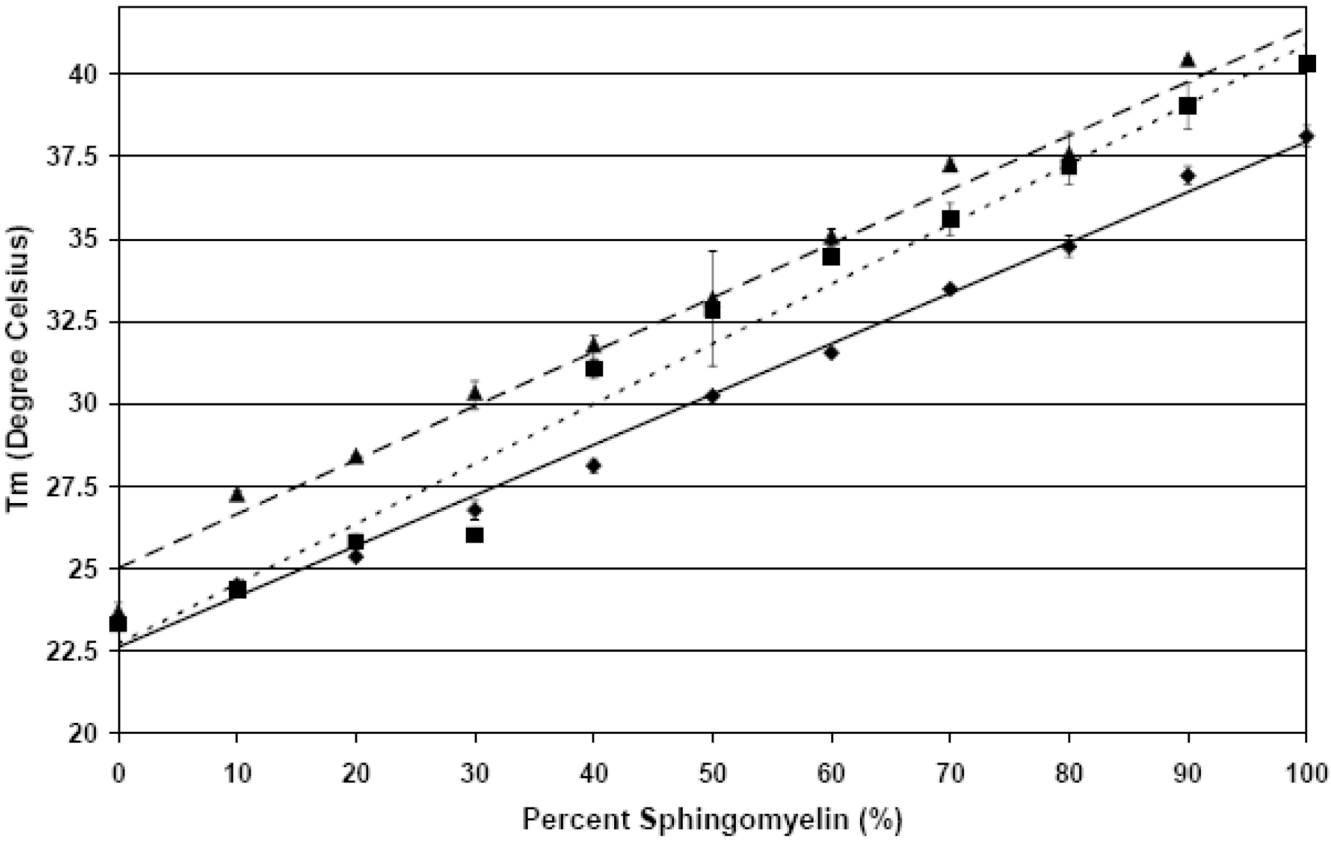

Figure 2.

The average melting temperature (Tm) of DMPC and SM liposomes of the L_α transition with and without apoLp-III measured. Shown are data points at 10% SM increments (± SE) and the corresponding trend line. (♦,——)) Average Tm liposomes; (▪,- - - - -)) average Tm for liposomes and apoLp-III; (▲, — — —) average Tm for liposomes and codissolved apoLp-III.

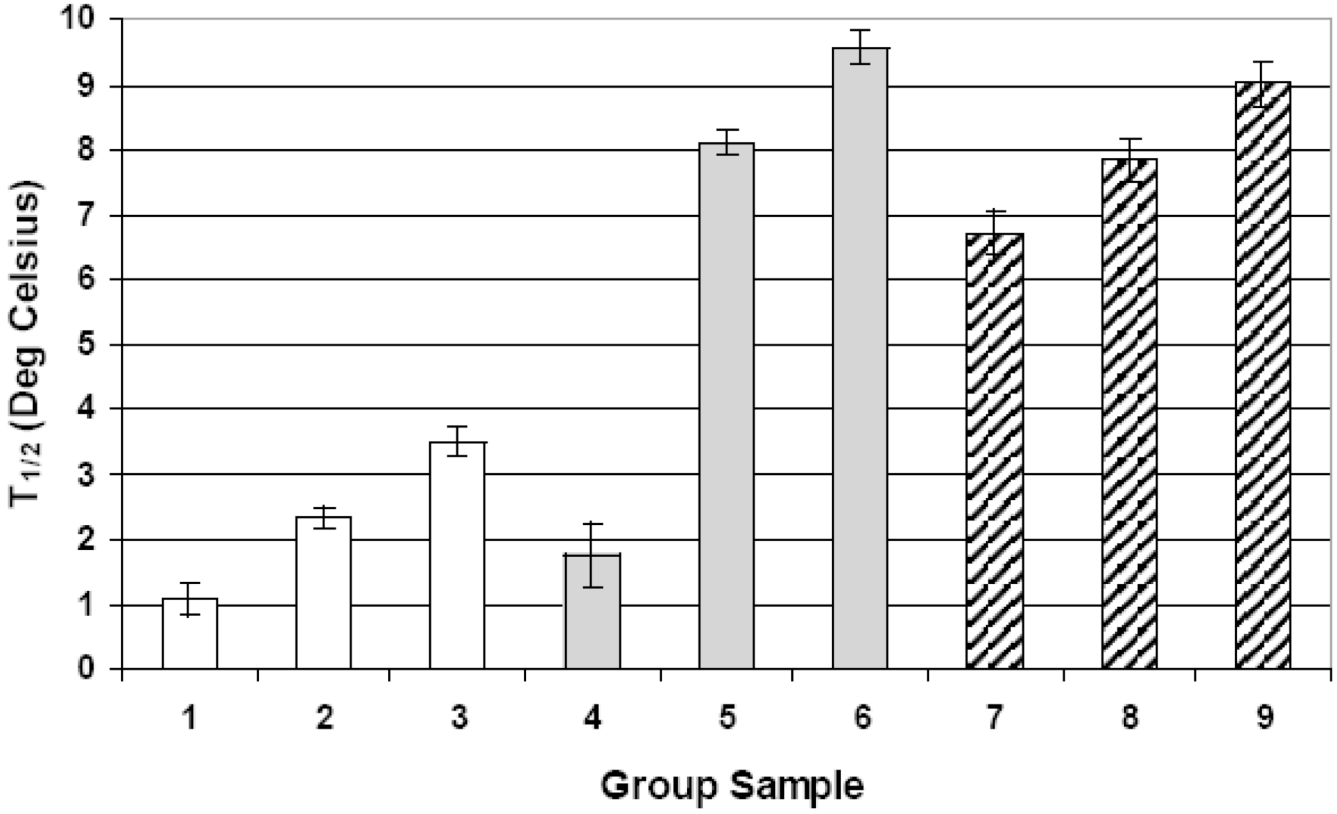

Figure 3.

Average $T_{1/2}$ of the L_α transition of the DMPC/SM liposomes. (□) liposomes; (■) liposomes and apoLp-III; (▨) liposomes and codissolved apoLp-III. Group 1: 0, 10, 20 %SM Group 2: 30, 90, 100 %SM Group3 40, 50, 60, 70, 80 %SM Group 4: 0, 10, 30 %SM Group 5: 20, 40, 50 90 %SM Group 6: 60, 80, 70, 100 % SM Group 7: 0, 10, 30, 90 % SM Group 8: 20, 70, 100 %SM Group 9: 40, 50, 60, 80% SM. All Data is show with ±SE

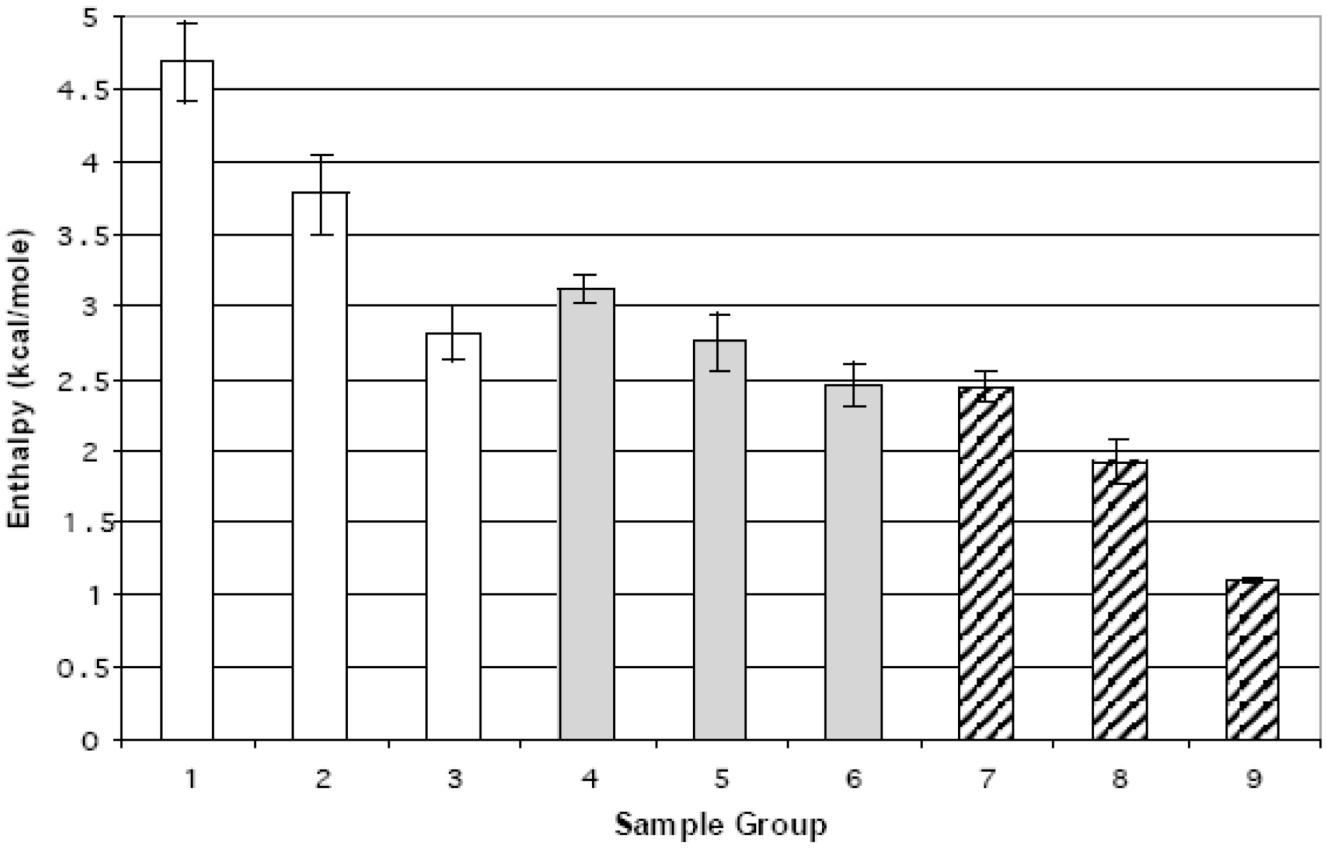

Figure 4.

Average enthalpy of the L_α transition of the DMPC/SM liposomes. (□)liposomes; (■) liposomes and apoLp-III; (▨) liposomes and codissolved apoLp-III. Group 1: 0, 20, 60, 80, 90, 100 %SM Group 2: 10, 40, 70 %SM Group 3 30, 50 %SM Group 4: 10, 20, 30, 80%SM Group 5: 40, 70 %SM Group 6: 0, 50, 60 90 100 %SM Group 7: 0, 20, 30, 40, 60, 80 % SM Group 8: 10, 50, 70, 100 %SM Group 9: 90% SM. Group 9 error bars represent the range between the maximum and minimum values.

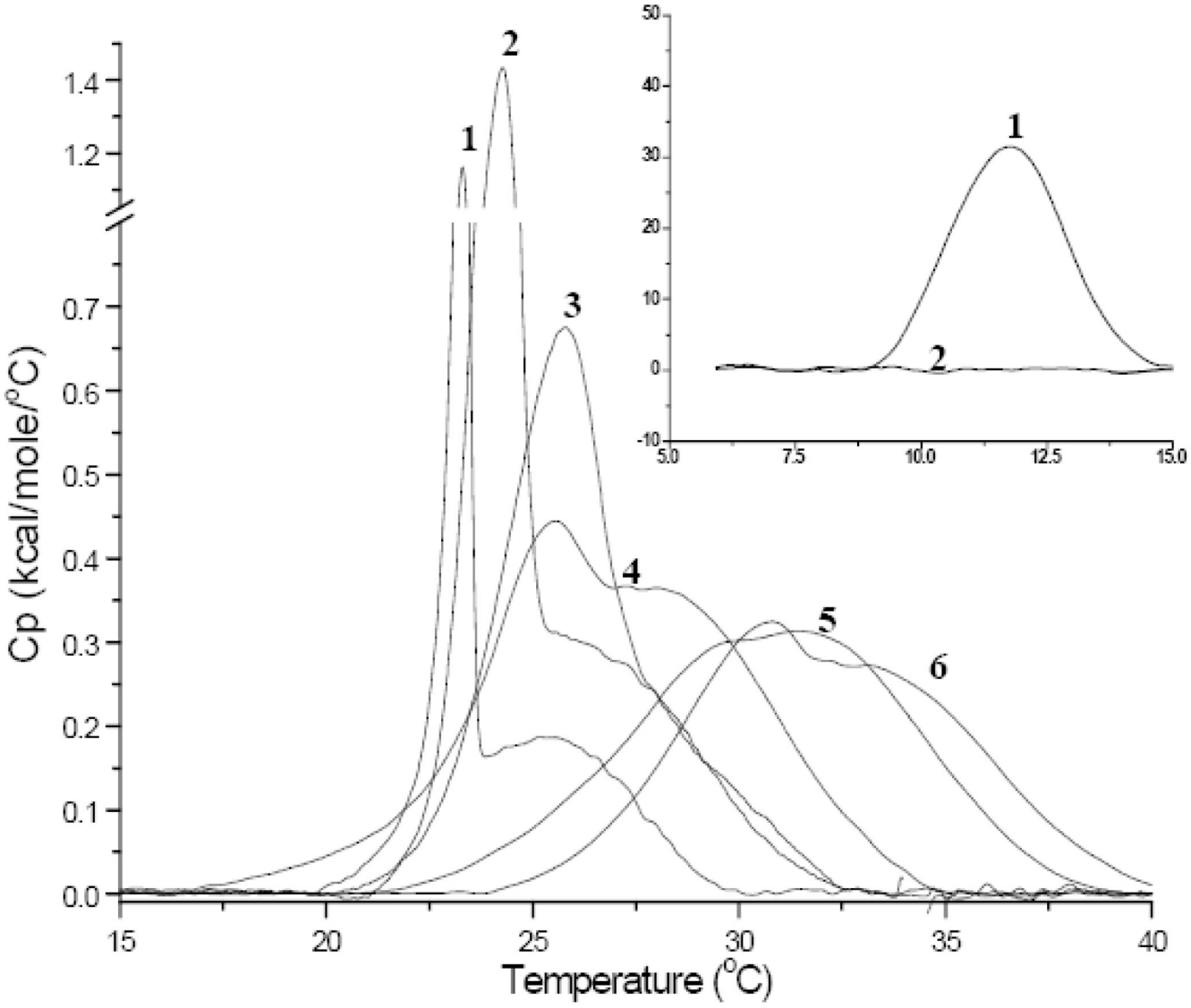

Figure 5.

DSC Heating Thermographs of MLVs of mixtures of DMPC and SM in the presence of apoLp-III 1) 100% DMPC 2) 80% DMPC and 20% SM 3) 60% DMPC and 40% SM 4) 40% DMPC and 60% SM 5) 20% DMPC and 80% SM 6) 100% SM. The insert shows the pre-transitional peak for 1) and 2) from 5 −15°C.

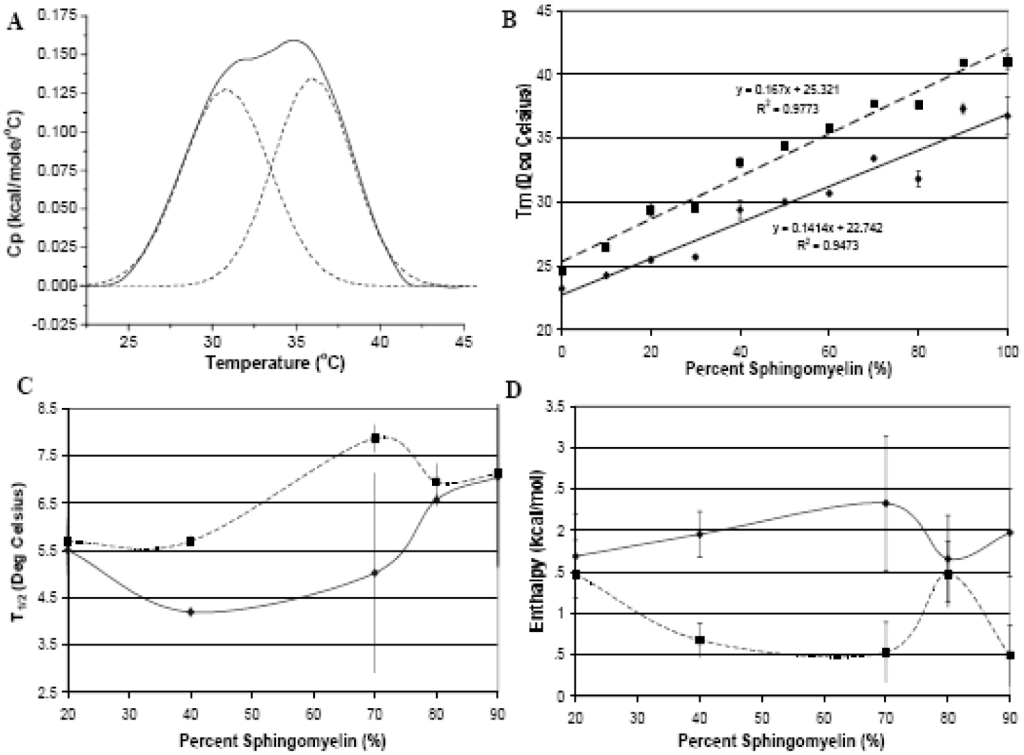

Figure 6.

2 Peak Gaussian Fittings for DMPC SM liposomes with apoLp-III (molar ratio 30:1). A) Curve Fitting of DSC heating scan of 20% DMPC and 80% SM with apoLp-III. B) 2 Peak Gaussian Fittings for Tm C) 2 Peak Gaussian Fittings for $T_{1/2}$ D) 2 Peak Gaussian Fittings for Enthalpy (▪) Peak 1 DMPC (♦) Peak 2 (SM) (——) Trend line for Peak 1 (---) Trend Line for Peak 2. All Values are shown are averages with the error bars representing the maximum and minimum values.

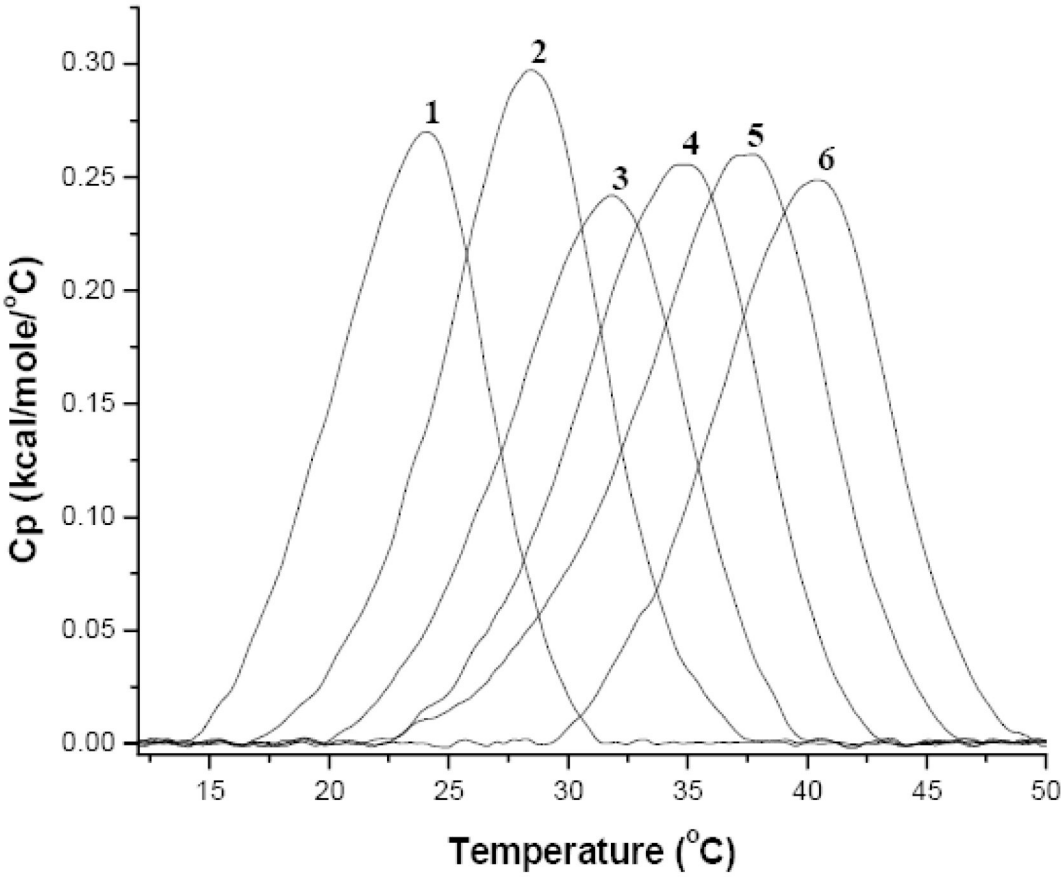

Figure 7.
DSC Heating Thermographs of MLV of mixtures of DMPC and SM (1mg/mL PBS) with codissolved apoLp-III. 1) 100% DMPC 2) 80% DMPC and 20% SM 3) 60% DMPC and 40% SM 4) 40% DMPC and 60% SM 5) 20% DMPC and 80% SM 6) 100% SM.

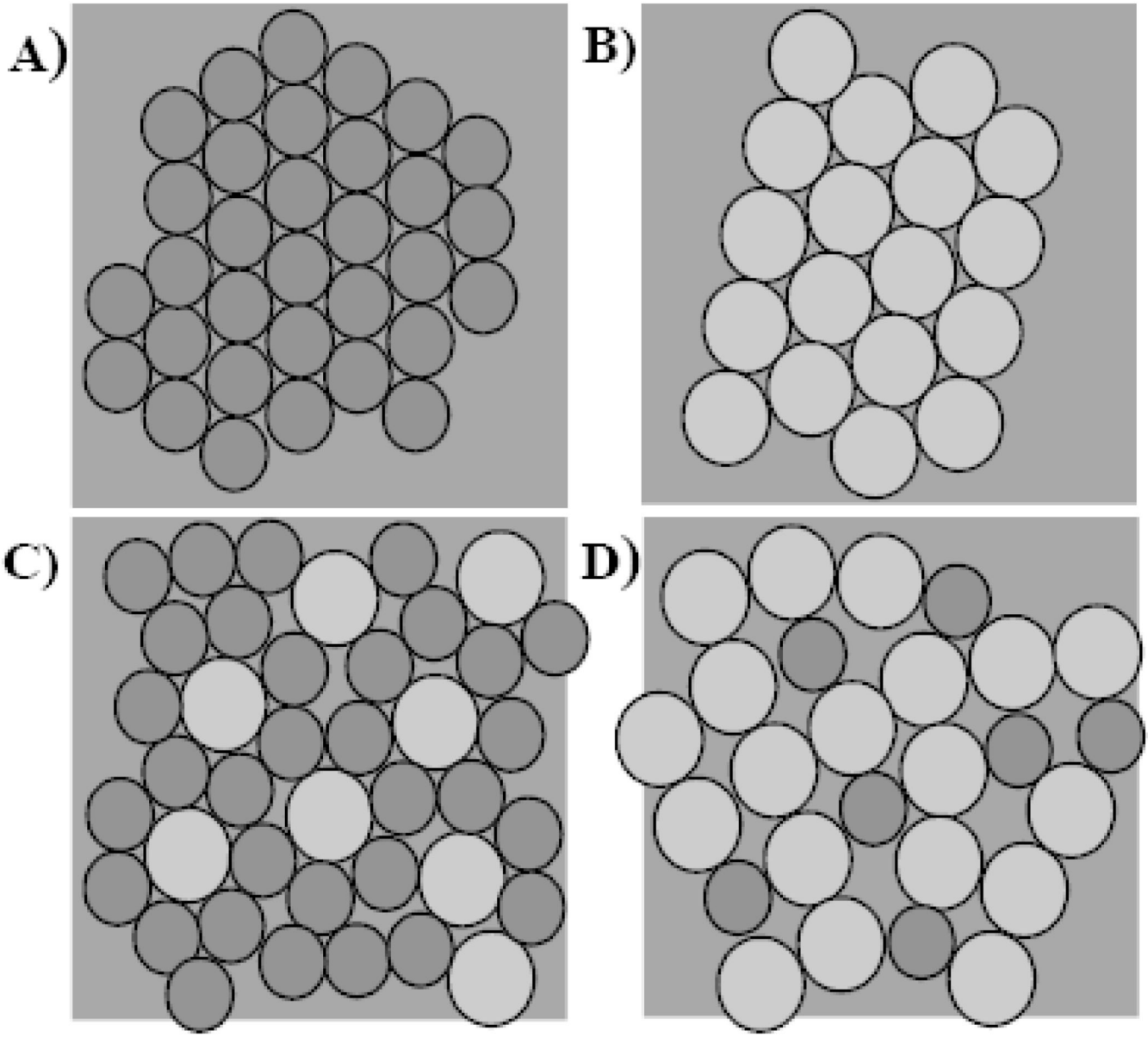

Figure 8.
Illustration of packing defects due to differences in lipid sizes. A) DMPC packing B) Sphingomyelin packing C) Smaller DMPC is capable of accommodating the larger sphingomyelin molecules. D) Small amount of DMPC in a sphingomyelin matrix creates more surface defects than in C (adapted from [26]).